International Research Journal of Emerging Trends in Multidisciplinary
ISSN 2395-4434
Volume 1, Issue 5 July 2015
www.irjetm.com

CORROSION BEHAVIOUR OF SINTERED 316L AUSTENITIC STAINLESS STEEL COMPOSITES

Mahaboob Patel[1], R Muthu Vaidyanathan[2], N Sivaraman[3]
1,2,3 Dept of Mechanical Engineering,
Wolaita Sodo University, Wolaita Sodo, Ethiopia.
Email: mpspatel@gmail.com

ABSTRACT:

Stainless steels are selected primarily for their excellent corrosion and oxidation resistance properties. One of the effective methods for manufacturing stainless steel parts of high quality and accuracy at low cost is through powder metallurgy. The demand for sintered stainless steels has increased notably, in the recent years due to their promising properties, ease of fabrication, and are economical in production, especially where number of complex objects are involved. The corrosion resistance of sintered stainless steel is poor due to their low density and high porosity, which in turn limits their use in most of the large scale parts production. Several studies have been carried in order to understand the properties of sintered stainless steels that are obtained using different methods.

The aim of the present work was to determine the corrosion behaviour of sintered 316L austenitic stainless steel (SASS) composites reinforced with powder oxides like Ga_2O_3, Nb_2O_5 and ZrO_2 powders. Powders were added in proportion of 1 wt% to 3 wt%. The mixtures were compacted into a cylindrical disc of 11mm diameter and 2mm thick at 70 kN. The so obtained compacts were sintered in lab (non-inert) atmosphere at 1250ºC for 30 minutes. The sintered compacts after SEM analysis were subjected to corrosion rate study by Tafel Extrapolation Method.

Keywords: Powder Metallurgy, Sinter, Corrosion, Stainless Steel, metal matrix composite

INTRODUCTION:

Powder metallurgical (P/M) stainless steels are increasingly being used for automotive and structural applications. Compared with the conventional cast and wrought route, P/M stainless steel can be processed at a lower temperature, can be near-net shaped, yields a greater material utilization (>95%), and has a more refined and homogeneous microstructure. Despite these advantages, P/M stainless steel has relatively poor corrosion resistance due to the presence of residual porosity. There is considerable scope for improving the properties of P/M components through novel sintering techniques and/or by alloying additives.[1]

P/M stainless steel is generally used in special applications, where enhanced properties are required as compared to the low alloy steel [2]. The P/M stainless steel consolidated by solid state sintering does not attain the full density and porosity as high as 15% is present [3]. Hence, in the recent years attempts have been made to attain the

full densification through the liquid phase sintering methods. The prealloyed stainless steel powders led to the super solidus liquid phase sintering (SLPS) which involves the heating of the prealloyed powder between the solidus and liquidus temperatures to form a liquid phase [4]. During supersolidus liquid phase sintering the fragmentation of the individual grains and rearrangement of these particles occurs followed by solution re-precipitation resulting in enhanced densification. The superior properties are attained through SLPS route due to the presence of the high diffusivity liquid allowing for rapid densification [3].

Liquid formation can be achieved through addition of the second phase dispersoids. Extensive studies have been carried out on yttria dispersed P/M stainless steel by Lal *et al* [5], which resulted in homogenous porosity. This was attributed to the interaction of Cr_2O_3 with Y_2O_3 dispersoids. The effect of SiC addition to P/M SS on sintering behaviour was investigated by Patankar and Tan [6] resulting in higher sintered density. Recently Shankar and Upadhyaya reported that an addition of greater than 5% yttria to P/M SS improves the sintered density appreciably [7]. Also it was shown by the Debata and Upadhyaya that the corrosion resistance of the nickel based super alloys improved due to the formation of yttrium aluminate [7].

The literature on the corrosion behaviour of P/M 316L SASS composites is very limited. There are no published reports on corrosion behaviour of 316L SASS composites reinforced with powder oxides like Ga_2O_3, Nb_2O_5 and ZrO_2. The present study was carried out to evaluate the corrosion behaviour of 316L austenitic stainless steel composites reinforced with powder oxides like Ga_2O_3, Nb_2O_5 and ZrO_2 processed by sintering in lab atmosphere at 1250°C in comparison with conventional sintered stainless steel.

EXPERIMENTAL WORK:

Materials:

Matrix and Reinforcements: Matrix is made up of PM 316L austenitic stainless steel, reinforcement oxides use areGa_2O_3, Nb_2O_5 and ZrO_2.

Table.1 Melting points of the reinforcement oxides.

Powder	**Melting Point**
Ga_2O_3	1900 ^oC (alpha), 1725 ^oC (beta)
Nb_2O_5	1512 ^oC
ZrO_2	2715^oC

Solution: 5 wt% NaCl in distilled water.

Mixing: 316L austenitic stainless containing 0-3 wt % oxide powders were mixed with mortar and pestle for 20 minutes.

International Research Journal of Emerging Trends in Multidisciplinary
ISSN 2395-4434
Volume 1, Issue 5 July 2015
www.irjetm.com

Compaction: The mixed powders were uniaxially compacted at 70 kN in a Universal Testing Machine (model UTN/E 40). To minimize friction, compaction was carried out using Zn stearate as a die wall lubricant.

Pellets dimensions: 11 mm diameter and 2 mm thick.

Fig. 1

Sintering: The green compacts were sintered at 1,250^{o}C for 30 min in lab (non-inert) atmosphere using conventional muffle furnace. The compacts were heated at a constant heating rate of 5°C/min and were allowed normalize by switching off the furnace.

Microstructural Analysis: The powder particle size and microstructural analysis of the sintered specimens were carried out using scanning electron microscope (model: JED 2300, Supplier: JEOL, Japan).

Corrosion Studies: Tafel polarization studies were carried out by using a potentiostat (Wenking Model LB 81) and a 3-electrode cell.

The surfaces of the samples were polished with 600 grit SiC papers before corrosion testing to produce a smooth surface finish followed by acetone cleaning to obtain cleaner surface. 6mm^2 surface areas of the polished specimens were exposed to 100 ml of 5% NaCl solution (prepared in distilled water) at room temperature.

The polarization studies were made from -250mV to +250mV vs. respective OCP with a scan rate of 20mV per minute and the corresponding corrosion currents, i, was recorded. From E Vs log I plot, E_{corr} and i_{corr} were determined. The corrosion rate (C.R), in mpy, is calculated using the relation:

$$\mathbf{C.R\ (mpy) = 0.0451\ x\ i_{corr}\ x\ E_w} \quad \text{.....(1)}$$

where i_{corr} is current density in $\mu A.cm^{-2}$ and E_w is Equivalent weight.

RESULTS AND DISCUSSION:

Particle Size and Shape: The average size and shape of the particles of 316L austenitic stainless steel powder used in the present work were measured and identified by scanning electron microscope; the mean average size was found to be 45microns. The shape of the particles is found to be irregular, which is the characteristic of water atomized powders.

International Research Journal of Emerging Trends in Multidisciplinary
ISSN 2395-4434
Volume 1, Issue 5 July 2015
www.irjetm.com

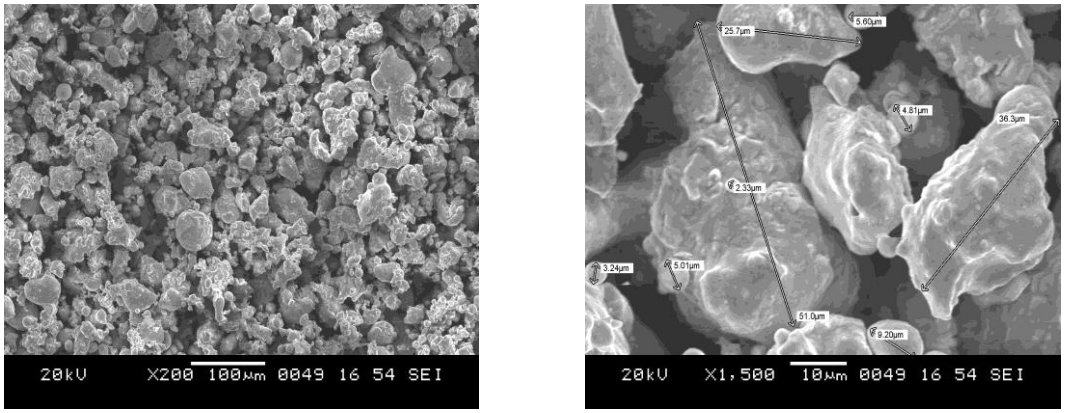

Fig.2 SEM images of stainless steel powder at 200X and 1500X.

Microstructures:

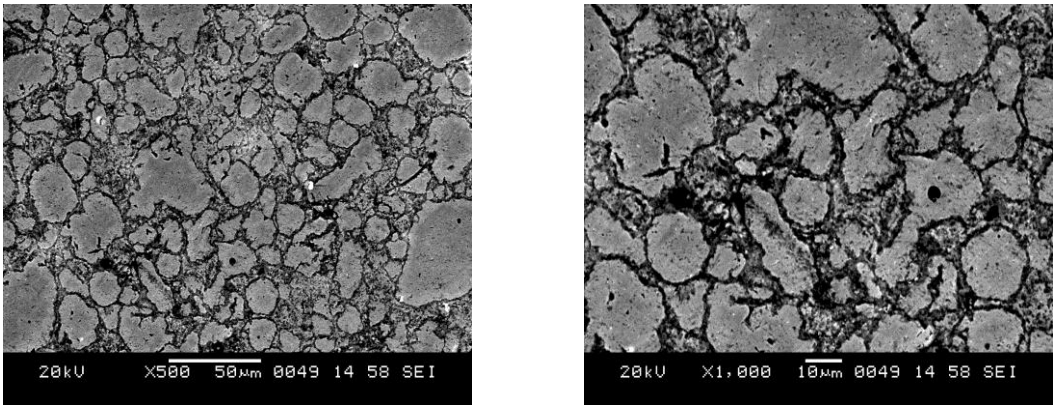

Fig.3 SEM images of plain 316L SASS at 500X and 1000X

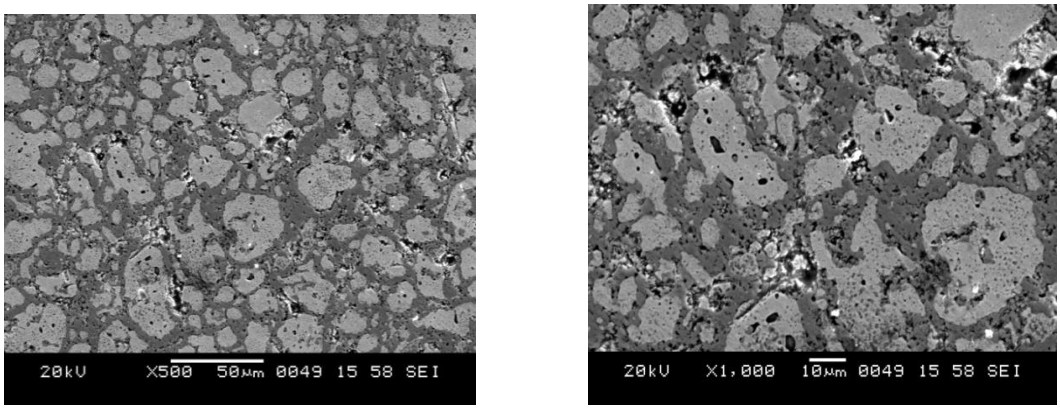

Fig.4 SEM images of 316L SASS composite with Ga_2O_3 at 500X and 1000X.

International Research Journal of Emerging Trends in Multidisciplinary
ISSN 2395-4434
Volume 1, Issue 5 July 2015
www.irjetm.com

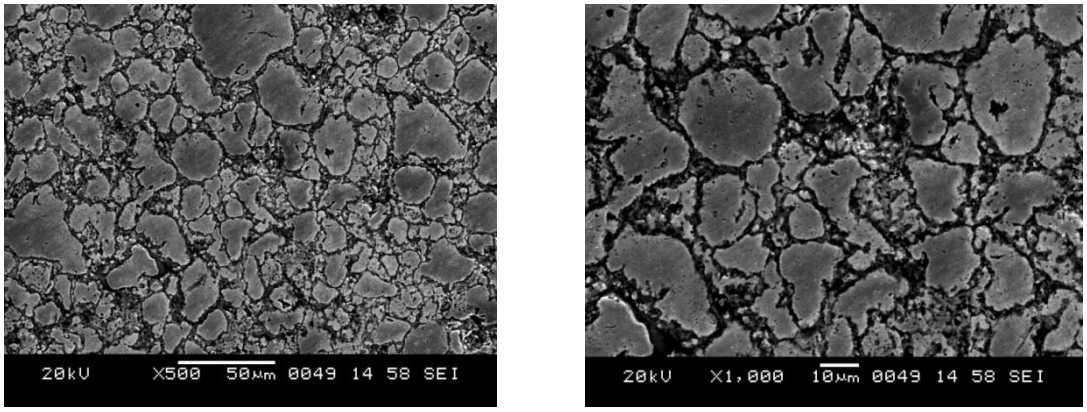

Fig.5 SEM images of 316L SASS composite with Nb_2O_5 at 500X and 1000X.

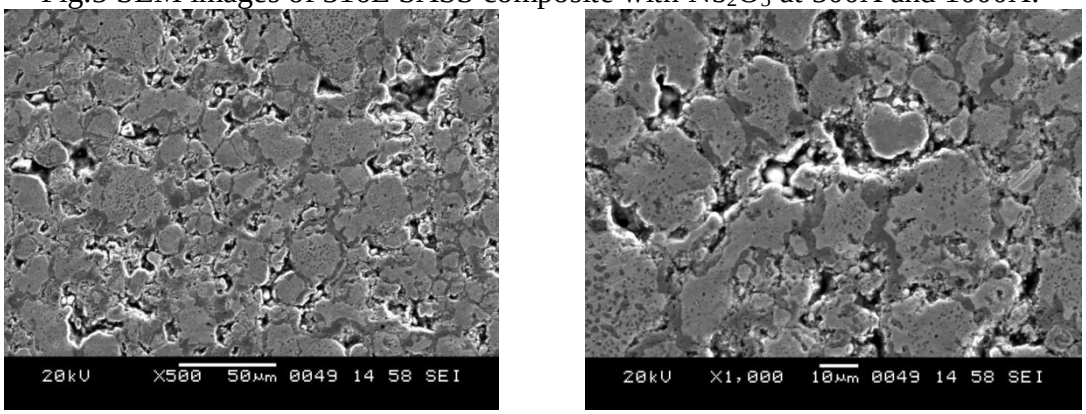

Fig.6 SEM images of 316L SASS composite with ZrO_2 at 500X and 1000X.

The SEM images reveal the pore profile of the sintered samples prepared for the present study. The microstructure of the 316L SASS composites shows increased porosity for the oxides with higher melting points as is seen in the above SEM images. Among the oxides used ZrO_2 has highest melting point of around 2715^oC and is obvious that, it would not form a liquid phase at sintering temperature which is required for the reduction of porosity, instead it obstructs the joining of adjacent metal particles resulting in increased porosity of the composite. Nb_2O_5 reinforced SASS shows a reduced porosity, which can be attributed to formation of semi-liquid phase at sintering temperature and thereby diffusing in the intergrannular spaces left during the sintering. Composites with Ga_2O_3 showed intermediate percentage of porosity and densification.

The Tafel's polarization curves obtained for plain and metal-oxide (Ga_2O_3, Nb_2O_5 and ZrO_2) reinforced composite samples are as shown below.

International Research Journal of Emerging Trends in Multidisciplinary
ISSN 2395-4434
Volume 1, Issue 5 July 2015
www.irjetm.com

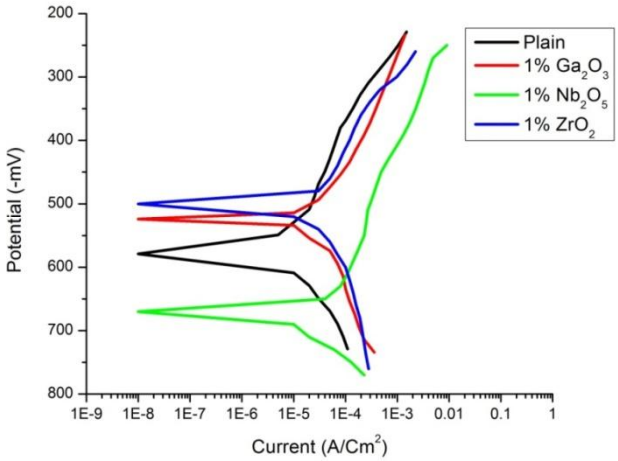

Fig.6 Polarization curves for 316L plain and SASS composites with 1% oxides

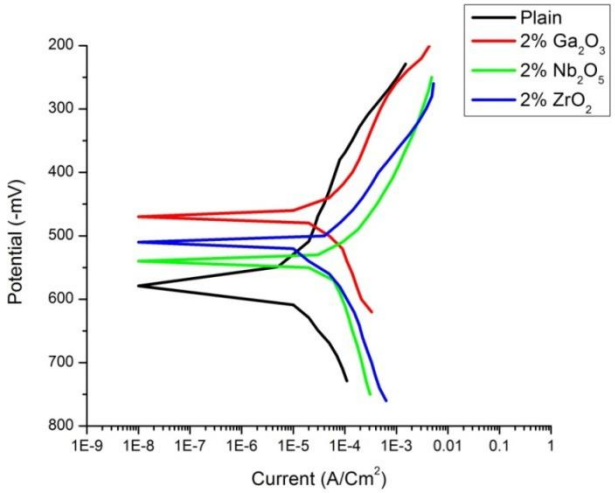

Fig.7 Polarization curves for 316L plain and SASS composites with 2% oxides

International Research Journal of Emerging Trends in Multidisciplinary
ISSN 2395-4434
Volume 1, Issue 5 July 2015
www.irjetm.com

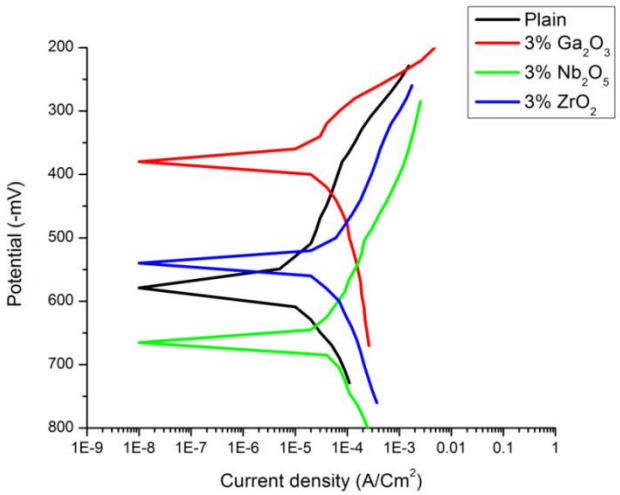

Fig.7 Polarization curves for 316L plain and SASS composites with 3% oxides

Table.2 Corrosion data (Tafel) calculated by using eqn.1

SI.NO	Sample	Composition	E_{corr} (-mV)	I_{corr} (A/Cm^2)	Corrosion Rate (mpy)
1	Plain	-	561	0.14	16.578
2	1GL	1% Ga_2O_3	546	0.41	49
3	1NL	1% Nb_2O_5	484	0.39	46.683
4	1ZL	1% ZrO_2	473	0.42	50.274
5	2GL	2% Ga_2O_3	470	0.62	74.214
6	2NL	2% Nb_2O_5	562	0.69	82.593
7	2ZL	2% ZrO_2	485	0.58	69.426
8	3GL	3% Ga_2O_3	243	0.64	76.608
9	3NL	3% Nb_2O_5	675	0.32	29.925
10	2ZL	3% ZrO_2	545	0.59	69.032

In order to have a clear cut idea about the variation of corrosion behaviour the corrosion rates for plain as well as composite samples are plotted using column chart as shown below.

International Research Journal of Emerging Trends in Multidisciplinary
ISSN 2395-4434
Volume 1, Issue 5 July 2015
www.irjetm.com

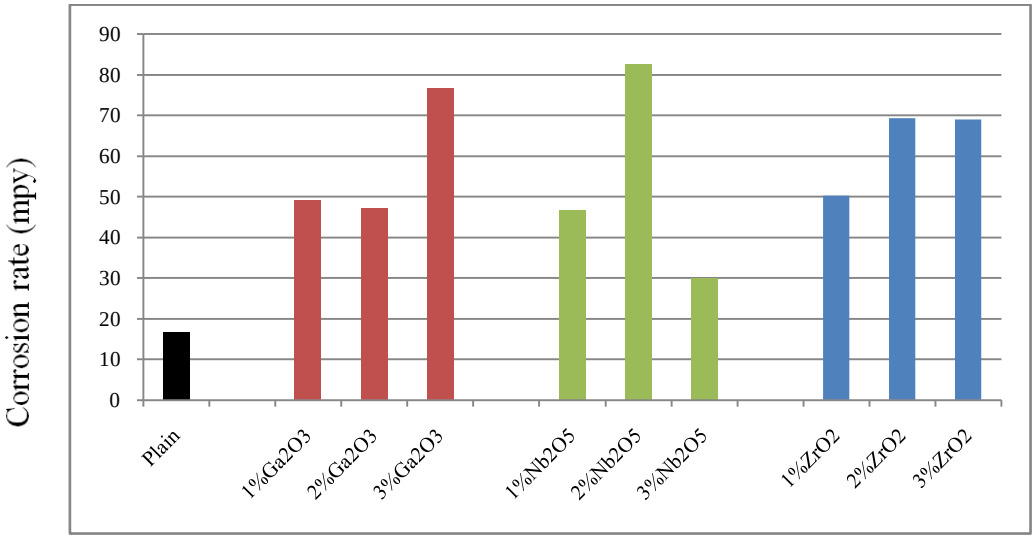

Fig.8 Corrosion rates of various 316L SASS samples

It is clear from the above column chart that, the SASS composites exhibits higher corrosion rates as compared to the plain sample.

But when corrosion rate is compared among SASS composites, it is observable that, the sample with 3% Nb_2O_5 exhibits lower corrosion rate. This can be attributed to the softening of Nb_2O_5 at sintering temperature thereby enhancing the densification of the sample. The densification entails closure of interconnected porosity. Consequently, the access of corrosive medium into pores is greatly reduced, which in turn reduces the corrosion rate.

On the other hand the high corrosion rate of the samples with Ga_2O_3 and ZrO_2 can be clearly understood by observing the SEM images which exhibits high percentage of porosity. The high melting point of Ga_2O_3 and ZrO_2 is reason which does not allow the sample to attain densification by obstructing the joining of adjacent metal particles. The particles of Ga_2O_3 and ZrO_2 occupy the inter-granular sites even after consolidation without forming secondary phase or compound with matrix; hence increase the interconnected porosity, which thereby allow the access of corrosive medium into pores.

Since the samples were sintered in lab atmosphere the corrosion rate of these samples did not show regularity in their behaviour. The lab atmosphere and the high melting point of the reinforcement oxides cause the poor compaction and appear to be the possible reason for the irregular corrosion behaviour and increased rate of corrosion.

CONCLUSIONS

According to achieved results, 316L SASS composites can be obtained starting from stainless steels powders by simple addition of metal oxides, through a common lab compaction and sintering process. Among manufactured composite samples the better densification and increased corrosion resistance was demonstrated by Nb_2O_5 reinforced composites. Furthermore, it is also evident from microstructure that Nb_2O_5 addition

results in a decrease sintered porosity. Both these factors result in the enhancement of corrosion resistance. On the other hand 316L SASS composites with Ga_2O_3 and ZrO_2 promoted increased porosity and poor densification and hence prone to high corrosion rate. However the attempt did not produce a composite with corrosion resistance better than plain 316L SASS. From the results obtained it can be deduced that, the better option to enhance the corrosion resistance is to use the reinforcement with melting point near to sintering temperature, which is expected to diffuse via capillary action to reduce the porosity and increased density.

REFERENCES

1. C. Padmavathi, A. Upadhyayaa, and D. Agrawal "Corrosion behavior of microwave-sintered austenitic stainless steel composites" Scripta Materialia 57 (2007) 651–654.
2. J.H. Reinshagen and A.J. Neupaver, "Fundamentals of P/M Stainless Steel", Powder Metallurgy Conference and Exhibition, San Diego, California (1989) 1-13.527
3. R.M. German, Sintering Theory and Practice, Wiley, New York, NY, USA, 1996.
4. R.M. German, Powder Metallurgy of Iron and Steel, Wiley, New York, NY, USA, 1998.
5. S. Lal, Sintering of 316L austenitic stainless steel–Y_2O_3 particulate composites, PhD Thesis, Indian Institute of Technology, Kanpur, India, 1988.
6. S.N. Patankar, M.J. Tan, Powder Metall. 43 (4) (2000) 350– 352.
7. M. Debata, G.S. Upadhyaya, Corrosion behavior of powder metallurgy Y2O3 dispersed iron- and nickel-basesuperalloys, J. Mater. Eng. Perform. 10 (2001) 602–607.
8. Clark DE, Sutton WH. Ann. Rev. Mater. Sci. 1996; 26:299.
9. Sutton WH. Ceram. Bull. 1989; 68:376.
10. Roy R, Agrawal DK, Cheng JP, Gedevanishvili S. Nature. 1999; 399:668.
11. R.M. Anklekar, D.K. Agrawal, and R. Roy, "Microwave Sintering and Mechanical Properties of P/M Steel", Powder Metal. Vol. 44[4], 355-362 (2001).,
12. R.M. Anklekar, K. Bauer, D. K. Agrawal and R. Roy, "Improved mechanical properties and microstructural development of microwave sintered copper and nickel steel PM parts," Powder Metallurgy, March 2005, vol. 48, no. 1, pp. 39-46.
13. S.S. Panda, V. Singh, A. Upadhyaya and D. Agrawal, "Sintering response of austenitic (316L) and ferritic (434L) stainless steel consolidated in conventional and microwave furnaces", Scripta Materialia, 54 (2006) 2179-2183.